Zeitschrift: Swiss bulletin für angewandte Geologie = Swiss bulletin pour la géologie appliquée = Swiss bulletin per la geologia applicata = Swiss bulletin for applied geology

Herausgeber: Schweizerische Vereinigung von Energie-Geowissenschaftern; Schweizerische Fachgruppe für Ingenieurgeologie

Band: 29 (2024)

Heft: 1-2

Artikel: Stress modeling for the AGEPP geothermal project in Lavey-les-Bains, Switzerland

Autor: Vescovi, Andrea

DOI: https://doi.org/10.5169/seals-1062149

Nutzungsbedingungen

Die ETH-Bibliothek ist die Anbieterin der digitalisierten Zeitschriften auf E-Periodica. Sie besitzt keine Urheberrechte an den Zeitschriften und ist nicht verantwortlich für deren Inhalte. Die Rechte liegen in der Regel bei den Herausgebern beziehungsweise den externen Rechteinhabern. Das Veröffentlichen von Bildern in Print- und Online-Publikationen sowie auf Social Media-Kanälen oder Webseiten ist nur mit vorheriger Genehmigung der Rechteinhaber erlaubt. Mehr erfahren

Conditions d'utilisation

L'ETH Library est le fournisseur des revues numérisées. Elle ne détient aucun droit d'auteur sur les revues et n'est pas responsable de leur contenu. En règle générale, les droits sont détenus par les éditeurs ou les détenteurs de droits externes. La reproduction d'images dans des publications imprimées ou en ligne ainsi que sur des canaux de médias sociaux ou des sites web n'est autorisée qu'avec l'accord préalable des détenteurs des droits. En savoir plus

Terms of use

The ETH Library is the provider of the digitised journals. It does not own any copyrights to the journals and is not responsible for their content. The rights usually lie with the publishers or the external rights holders. Publishing images in print and online publications, as well as on social media channels or websites, is only permitted with the prior consent of the rights holders. Find out more

Download PDF: 04.02.2026

ETH-Bibliothek Zürich, E-Periodica, https://www.e-periodica.ch

Stress modeling for the AGEPP geothermal project in Lavey-les-Bains, Switzerland

Andrea Vescovi[1], MSc Thesis

Abstract
Deep borehole planning and exploitation must incorporate extensive knowledge of the in-situ stress state. Topographical structures can significantly alter gravity, tectonic deformation, and other sources of stress in the Earth's crust, and their impact can be felt up to 100 kilometers away (Heidbach et al., 2007). Understanding the stress state is crucial for evaluating borehole stability, productivity, and the risk of induced seismicity. Prior to drilling, it's advantageous to assess the stress tensor along the virtual well path to determine the optimal borehole configuration for safe and sustainable geothermal energy utilization.

1 Introduction

The AGEPP (Alpine Geothermal Power Production)'s deep geothermal project in Lavey-les-Bains (VS) is outlined as follows:

- Project overview: the project is the Switzerland's first geothermal energy venture, designed to generate both heat and electricity.
- Production goals: the target is to extract 40 L/s of hot water, with a temperature of around 110°C.
- Energy output: the extracted hot water will be used to produce 4.2 GWh of electricity and 15.5 GWh of thermal power.
- Impact: the electricity generated is sufficient to power 900 buildings. The thermal power will be used to heat the pool thermal water as well as buildings.
- Aquifer characteristics: the rock formation is a naturally fractured and highly permeable crystalline rock (fractured gneiss) (Sonney, 2007). The surrounding lakes replenish the aquifer. Hence, hydraulic stimulation is not required; only a possible de-calcification process to improve water flow from fractures to the borehole.
- Drilling strategy: initially, the borehole is excavated vertically; then it is deviated to increase the likelihood of intersecting major fractures. The total depth corresponds to 2957 m true vertical depth (TVD).

The goal of this work is to evaluate a reliable stress state around the geothermal site, by recognizing the importance of topographical effects on the stress conditions around the

[1] Pini Group, andrea.vescovi@pini.group

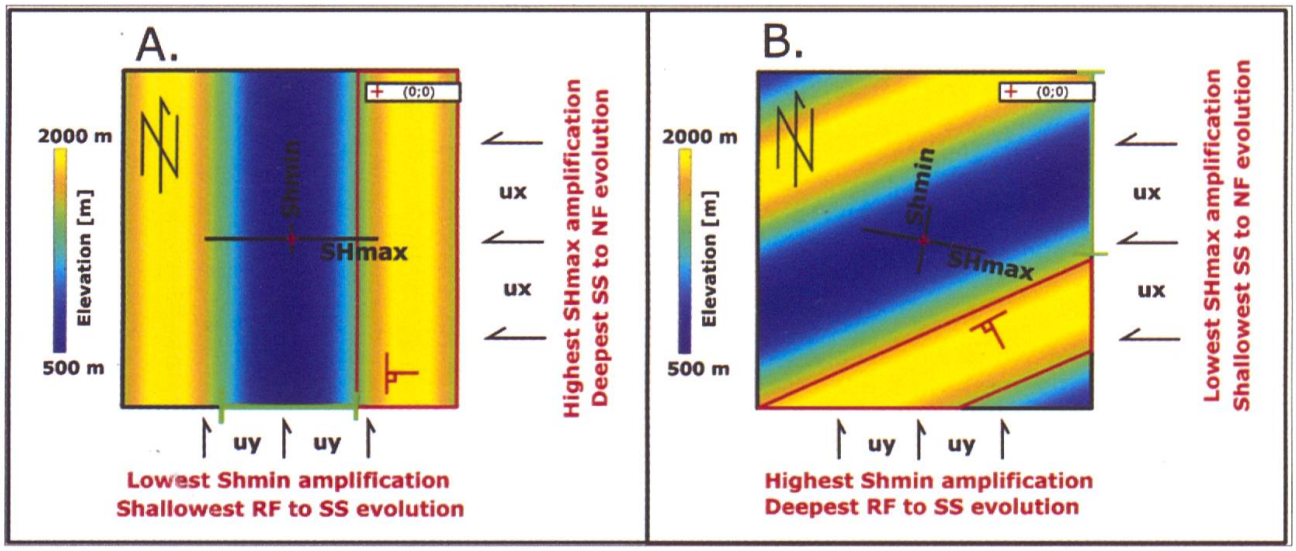

Fig. 1: Topographical effects mechanism on stresses distribution: topographical surface, view from top. Ridges framed in red, valley in green; crosses represent the stress ellipsoid (here in form of SHmax and Shmin components); black arrows represent the maximum *ux* and the minimum *uy* tectonic strains. **A.** Valley long axis orthogonal to the maximum horizontal tectonic; **B.** Valley long axis nearly orthogonal to the minimum horizontal tectonic strain.

LAVEY-1 borehole. The topography of the Rhône Valley is highly variable and its impact on the in-situ stress state is a key challenge. A 3D geomechanical numerical model with finite elements is employed, since this method accounts for structural heterogeneity (i.e., topographical surface), crucial for capturing local to regional variations in the stress field.

The research is structured around several key research questions, including 1) examining the qualitative impact of topography on stress regimes, 2) identifying the directions and magnitudes of maximum and minimum horizontal stresses along the LAVEY-1 borehole, 3) exploring whether topographical effects can be described with a first-order analytical stress state solution, 4) determining the magnitudes of the principal stresses according to the best-fitted 3D geomechanical numerical model, and 5) evaluate the consequences for borehole stability.

2 Analysis of topography's qualitative effects on stress regimes

The total effect of the topography on the state of stress can be obtained by adding the effect of gravitational stress with the effect of tectonic stress (Liu and Zoback, 1992). Topographical effects can have significant impact on the magnitude and direction of stresses at shallower depths (Warpinski and Teufel, 1991).

Topographical effects generate a significant amplification of SHmax and Shmin near the valley bottom. The incidence angle of horizontal tectonic strain directions on topographical structures is the driving factor for stress amplification and induced rotation. Ridges and valley complexes can greatly increase major horizontal stress magnitudes compared to flat regions, impacting stresses state at depths of more than one kilometer.

The greatest amplification depends on whether the maximum or minimum horizontal tectonic strain direction is orthogonal to the valley long axis. At the bottom of valleys parallel to maximum strain, maximum ampli-

fication of Shmin occurs, while maximum amplification of SHmax occurs in valleys orthogonal to maximum tectonic strain. If tectonic strains are not parallel to the valley's long axis, stress rotations will occur at shallower depths too. In this situation, Shmin follows 90° away from SHmax, which aligns itself towards the major ridges. Induced stress rotation may exceed 25°.

Stresses amplification can result in a strongly compressive faulting system (i.e., reverse faulting) that may not exist in flat morphology lands. Higher stress magnitudes are produced by deeper valley depressions and greater horizontal tectonic strains, which may result in ruptures close to the valley bottom. Figure 1 summarizes the topographical effects mechanism on stresses distribution.

The findings are directly assessed by the current work by qualitative 3D geomechanical modeling and confirmed by literature (Liu and Zoback, 1992; Warpinski and Teufel, 1991; Zang and Stephansson, 2010; Savage et al., 1985; Miller and Dunne, 1996; Pan et al., 1995; Savage and Morin, 2002).

At the LAVEY-1 borehole location, intense ridge effects and stress reorientation are expected at shallower depths. Topographical effects should be considered when assessing stresses state, particularly around the LAVEY-1 borehole.

3 Directions of maximum and minimum horizontal stresses along the LAVEY-1 borehole

The stress concentration around a borehole in rock formations varies based on distance and position relative to the borehole wall. The wall's response depends on both the stress field and rock strength. Stress concentration can result in tensile failures known as drilling-induced tensile fractures, or compressive failures known as breakouts. Drilling-induced tensile fracture happen when the lowest effective stress on the wall of the borehole is lower than the tensile strength (influencing factors are large deviatoric stress, correspondence between minimum principal stress and minimum effective stress, mud weight and wall cooling).

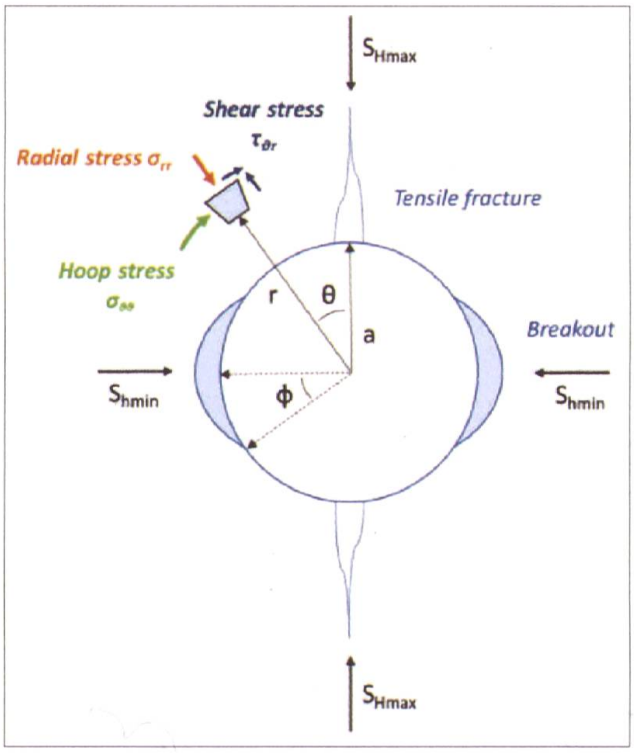

Fig. 2: Stresses concentration at the borehole wall (Koumrouyan, 2019). As the wellbore wall is a free surface, the principal stress trajectories are parallel and perpendicular to it. In case of vertical well, the zone of maximum compression is found at the azimuth of Shmin, and the zone of minimum compression is found at the azimuth of SHmax (Zoback, 2007).

Analysis of breakouts and drilling-induced tensile fractures help determine stress azimuths. As illustrated in Figure 2, in a vertical borehole, breakouts indicate the direction of minimum horizonal stress, while drilling-induced tensile fractures indicate the direction of maximum horizontal stress (Valley, 2007; Zoback, 2007).

Induced failure analysis of the LAVEY-1 borehole is performed to define principal horizontal stress direction and magnitude. The

analysis is carried out evaluating field data derived from Well Geometry Instrument (WGI, or oriented multi-arm caliper tool), acoustic, sonic and temperature log, to define stresses direction, induced stresses rotation by topographical effects, to constrain stresses magnitude at depth (i.e., with formation integrity tests), and finally to characterize a state of stress.

The analysis of induced failure confirms stresses rotation along the LAVEY-1 borehole, influenced by topographical effects. The first consistent shallower data on breakout azimuths are found between 500 and 600 m TVD. Breakouts azimuths are aligned with the Rhône Valley long axis, yielding Shmin direction of 163°. SHmax, which is 90° away (73°) from the breakouts azimuth, is thus perpendicular to the Rhône Valley long axis (Figure 3).

The SHmax mean directions is 111° in the second section of the borehole (594 - 1799 m TVD), 123° in the third section (1799 - 2100 m TVD), and 125° in the fourth section (2100 - 2957 m TVD). The regional far-field SHmax direction is reached approximately at 2'950 meters depth.

Furthermore, the LAVEY-1 induced rupture analysis reveals a reduction of breakouts severity from the surface up to 1'000 meters. These stress records confirm that horizontal stresses are significantly enhanced at the valley bottom.
The gravitational effects of massive ridge such as Dents de Morcles and Dents du Midi cause significant compression at the Rhône Valley bottom. This severe compression causes horizontal stresses to re-orient.

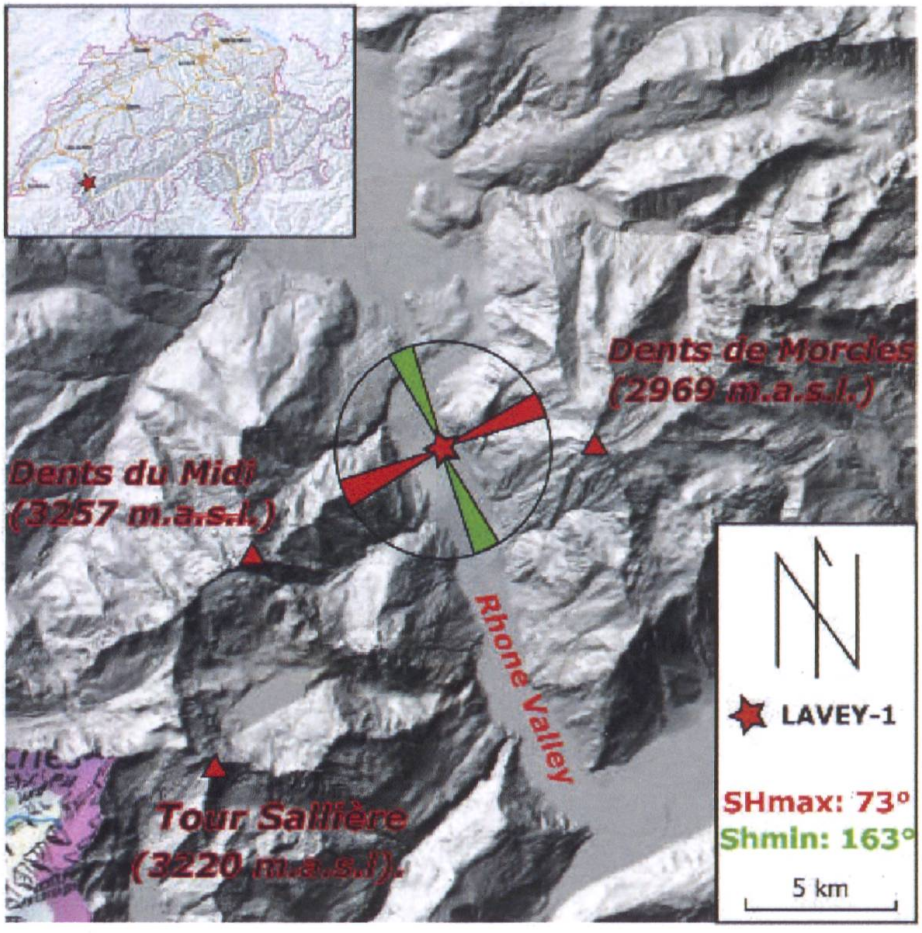

Fig. 3: Principal horizontal stresses direction between 500 and 600 meters depth beneath Lavey-les-Bains (VD). SHmax direction corresponds to 73° and Shmin direction corresponds to 163°. Shmin direction runs parallel to the Rhône Valley, while SHmax direction runs perpendicular to it. Topographical effects dictate stresses direction at shallow depth.

4 Characterize the state of stress in accounting for topographical effects

Strong compression is induced at the bottom of the Rhône Valley by the gravitational effects of nearby ridges, and the stresses magnitude at shallow depths cannot be quantified using a 1st order stress state characterization (or linear trends of stresses as a function of depth). Besides the strike-slip regional faulting stress regime reported in the literature (Kastrup et al., 2004; Heidbach et al., 2016), topographical structures may amplify the magnitude of several Mega-Pascals principal horizontal stresses, which can lead to a local reverse-faulting stress regime taking over in the first hundred meters of depth.

The *Compute Borehole Failure* function idealized by Dahrabou et al. (2022) is inversed to calibrate the breakouts width 2ϕ and extent eBO, the key borehole failure parameters, against the observation data gathered by logging to define the state of stress. Two formation integrity tests (FITs) conducted along the borehole and studies on the regional stress states (such as the Nant de Drance (VS) geotechnical research (NantDeDrance, 2022)) serve as the starting point from which the inverse function can start the minimizing procedure.

Since the breakouts width decreases from 600 to 1000 m TVD (amplification of compressive topographical effects towards the valley bottom), the inverse calibration begins at 1000 m TVD depth in attempting to limit the zone in which horizontal stresses cannot be characterized by a 1st order analytical solution.

To validate (or reject) this first essay, 3D numerical modeling is required, to consider topographical effects.

The topography surrounding Lavey-les-Bains is introduced in RS3 (Rocscience, 2022) from swissALTI3D (2022), with LAVEY-1 borehole at its center. Then, in assuming only gravity and tectonic acting as a source of stress on the 3D model, the gravity condition is firstly defined (body force), and lateral displacement boundary condition (surface horizontal forces, or horizontal tectonic strains) are consequently introduced.

The steps concerning the calibration of the 3D model correspond to (modified after Reiter and Heidbach, 2014):

1) Fixing the SHmax direction (sides walls orientation). SHmax direction corresponds to the one evaluated in the fourth section of the LAVEY-1 borehole (125°) because the model construction calls for undisturbed state of stress (it is assumed that topography has no longer effects along the last section of the borehole).
2) Identifying the best-fit kinematic boundary conditions. In the absence of stress data from in-situ measurements such as LOTs (Leak-Off Tests), kinematic boundary conditions are manually calibrated (with a *trials and errors* procedure, in which various scenarios are evaluated). The calibration uses the findings of FITs to determine the lower limits of vertical stress (SV) and minimum horizontal stress (Shmin).
3) Assessing best-fitted 3D geomechanical numerical model through failure simulation along the borehole. Adequate calibration is achieved when the simulated induced rupture (MATLAB computation from 3D model outputs) aligns well with observed induced rupture along the LAVEY-1 borehole (Annex for illustration).

Proposed Scenario	Stress regimes and principal stresses trend
A. **From borehole failure**	Strike-slip faulting stress regime:
	$S_V = 0.0265 \cdot TVD$ [MPa]
	$S_{Hmax} = 0.0355 \cdot TVD + 1.6706$ [MPa]
	$S_{hmin} = 0.0204 \cdot TVD - 0.0190$ [MPa]
B. **From 3D stress model**	Reverse faulting stress regime up to 495 meters TVD:
	$S_V = 2.8741 \cdot 10^{-7} \cdot TVD^3 - 2.9120 \cdot 10^{-4} \cdot TVD^2 + 0.1212 \cdot TVD + 1.9387$ [MPa]
	$S_{Hmax} = -2.0467 \cdot 10^{-7} \cdot TVD^3 + 2.3923 \cdot 10^{-4} \cdot TVD^2 - 0.0891 \cdot TVD + 50.7427$ [MPa]
	$S_{hmin} = -1.3557 \cdot 10^{-7} \cdot TVD^3 + 1.5643 \cdot 10^{-4} \cdot TVD^2 - 0.0517 \cdot TVD + 29.1726$ [MPa]
	Strike-slip from 495 to 1'190 meters TVD & Normal faulting stress regime below:
	$S_V = 0.0300 \cdot TVD + 10.2499$ [MPa]
	$S_{Hmax} = 0.0083 \cdot TVD + 36.3952$ [MPa]
	$S_{hmin} = 0.0091 \cdot TVD + 21.3197$ [MPa]

Tab. 1: Stress state characterization around the LAVEY-1 borehole.

5 Magnitudes of the principal stresses around the LAVEY-1 borehole

For the description of the stress situation around the LAVEY-1 borehole, two final scenarios are reported. One of them deals with the 1st order analytical solution for the stress state characterization using inverse calibration on borehole failure observation (A., Table 1 and Figure 4). The second is a numerical solution that corresponds to the stress tensor of the best-fitted 3D geomechanical numerical model (B., Table 1 and Figure 4).

When compared to the first-order analytical solution, the 3D geomechanical numerical

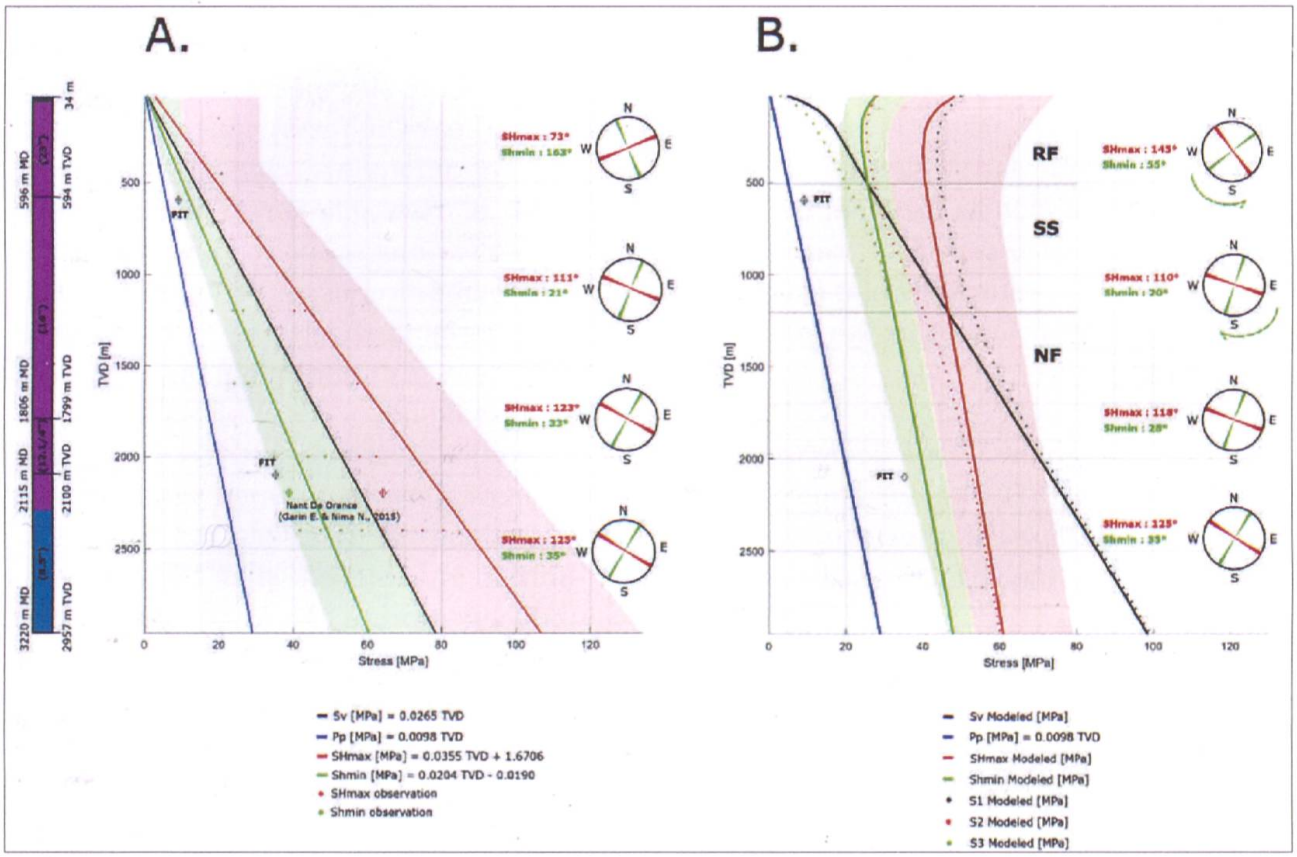

Fig. 4: Comparison between stress state characterized from borehole failure analysis and stress state characterized from the 3D geomechanical numerical model, along the LAVEY-1 borehole. A. Stress state characterized from LAVEY-1 borehole failure analysis (1st orderd analytical solution). B. Stress state characterized from the best-fitted 3D geomechanical numerical model (numerical solution).

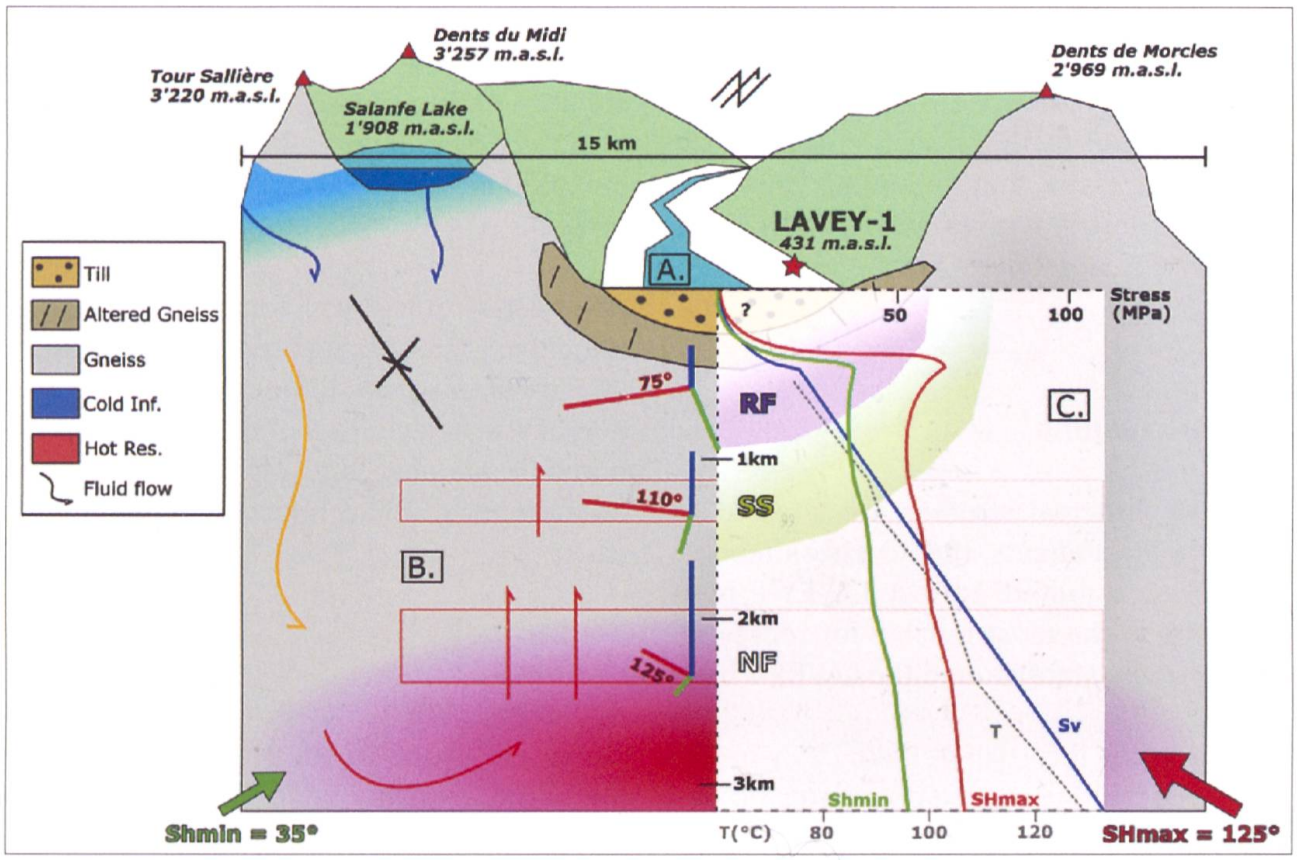

Fig. 5: Conceptual model of the state of stress beneath Lavey-les-Bains (VD) and surroundings. In A., the focus is on the Rhône Valley bottom, where till settled above the altered gneiss. This latter suffers the most from the induced strong compression and it undergoes to rupture. In B., the focus is on the rising hot geothermal water, which could cause horizontal compressive thermal stresses. Finally, in C., the stress state is conceptualized, modifying the best 3D stress model result in accounting for glacial and thermal effects.

model calibrated on LAVEY-1 data shows a consistent variation in the stress state around the borehole. The 3D stress model shows that topographical structures in the Lavey-les-Bains context have a strong influence. Up to 500 meters below the surface, a reverse faulting regime predominates, while a normal faulting stress regime can be found at approximately 1'000 meters depth.

The 3D numerical solution represents a more accurate stress tensor as it considers topographical effects on local stresses around the borehole. The calibrated 3D stress model is a reliable predictor of the stress state along the LAVEY-1 borehole. The added value derived from its application is a careful examination of the imposing topographical structures soaring up the flanks of the Rhône Valley.

However, the 3D stress tensor calibrated against LAVEY-1 data has some limitations. There is a mismatch between the simulated and the observed breakouts azimuth in the first section (form 0 up to 600 m TVD, Annex). In fact, the best-fitted 3D stress tensor is the result of a purely elastic model, in which a homogeneous material is applied everywhere. As a result, neither the rupture at the compressed valley bottom, the glacial effects (between 100 and 200 meters of till settling above the U-shaped valley), nor the temperature gradient could be evaluated.

Figure 5 conceptualizes the stress state as determined by the 3D best stress model considering potential glacial (A.) and thermal (B.) effects.

The borehole stability evaluations suggest deviating the borehole towards the direction of minimum horizontal stress (N 035°)

at around 2,000 meters TVD, with an inclination of 40°. Optimal fracture crossing occurs in the N 035° 40 direction. Additionally, fractures oriented in this direction exhibit the least compression and potentially larger apertures. These fractures would allow water to enter the borehole with the highest flow rate.

6 Conclusions

Since all principal stresses are affected by topographical effects, the 3D stress model's response calibrated against LAVEY-1 borehole data is the most reliable for representing the stress state around the LAVEY-1 borehole.

A reverse faulting regime dominates up to a depth of 500 meters. The component with the greatest uncertainty is SHmax, but an upper range is defined thanks to the manual calibration, and this indicates a maximum depth for the evolution to normal faulting stress regime, corresponding approximately at 2'000 meters.

To constrain analytical solutions, a deeper comprehension of the local stress state prior to drilling activity, and in-situ stress measurements (i.e., LOT) are required. Furthermore, key challenges such as stress regimes evolution intervals (i.e., when SHmax and Shmin are close to SV) are impossible to assess with model-independent data alone (Reiter and Heidbach, 2014), and only numerical models can indicate reliable evolution ranges. Other complexities for analytical solutions emerge at shallower depths, where a third-order polynomial expression is required to approximate the stress state (i.e. reverse faulting stress regime).

In conclusion, stresses magnitudes and stresses directions are strongly influenced by topographical structures in Lavey-les-Bains, particularly at shallower depths. Neglecting topographical considerations has undoubtedly adverse effects on borehole stability, and misinterpretations of the state of stress may have consequences for the potential rentability of the deep geothermal system.

The best 3D numerical solution provided is critical in (1) assessing topographical effects on local stress state, (2) indicating the evolution of stress regimes in depth, (3) assessing borehole stability, and (4) determining the orientation of SHmax if an EGS is planned.

7 Outlooks

Hydraulic tests for in-situ stress measurements are recommended because they improve the reliability of 3D numerical models and give constraints for analytical solutions. Future research should also include incorporating more local stress data, improving material representation and implementation of a plastic numerical model. Thermal effects and till settling in the U-shaped valley may be employed to increase model accuracy and reliability next to the surface.

References

Dahrabou, A., Valley, B., Meier, P., Brunner, P. & Alcolea, A. 2022: A systematic methodology to calibrate wellbore failure models, estimate the in-situ stress tensor and evaluate wellbore cross-sectional geometry. International Journal of Rock Mechanics and Mining Sciences 149:104,935, DOI 10.1016/j.ijrmms.2021.104935, URL https://linkinghub.elsevier.com/retrieve/pii/S1365160921003191 .

Heidbach, O., Reinecker, J., Tingay, M., Müller, B., Sperner, B., Fuchs, K. & Wenzel, F. 2007: Plate boundary forces are not enough: Second- and third-order stress patterns highlighted in the World Stress Map database: WORLD STRESS MAP DATABASE RELEASE 2005. Tectonics 26(6):n/a–n/a, DOI 10.1029/2007TC002133, URL http://doi.wiley.com/10.1029/2007TC002133 .

Heidbach, O., Rajabi, M., Cui, X., Fuchs, K., Müller, B., Reinecker, J., Reiter, K., Tingay, M., Wenzel, F., Xie, F., Ziegler, MO., Zoback, ML. & Zoback, M. 2018: The world stress map database release 2016: Crustal stress pattern across scales.

Tectonophysics 744:484–498, DOI https://doi.org/10.1016/j.tecto.2018.07.007 , URL . https://www.sciencedirect.com/science/article/pii/S0040195118302506 .

Kastrup, U., Zoback, ML., Deichmann, N., Evans, KF., Giardini, D. & Michael, AJ. 2004: Stress field variations in the Swiss Alps and the northern Alpine foreland derived from inversion of fault plane solutions: STRESS FIELD IN SWITZERLAND. Journal of Geophysical Research: Solid Earth 109(B1), DOI 10.1029/2003JB002550, URL http://doi.wiley.com/10.1029/2003JB002550 .

Koumrouyan, M. 2019: Geomechanical characterization of geothermal exploration borehole. Master's thesis.

Liu, L. & Zoback, MD. 1992: The effect of topography on the state of stress in the crust: Application to the site of the Cajon Pass Scientific Drilling Project. Journal of Geophysical Research 97(B4):5095, DOI 10.1029/91JB01355, URL http://doi.wiley.com/10.1029/91JB01355 .

MathWorks 2022: MATLAB, Official Site. https://www.mathworks.com/products/matlab.html

Miller, DJ. & Dunne, T. 1996: Topographic perturbations of regional stresses and consequent bedrock fracturing. Journal of Geophysical Research: Solid Earth 101(B11):25,523–25,536, DOI 10.1029/96JB02531, URL http://doi.wiley.com/10.1029/96JB02531 .

NantDeDrance 2022 : Nant de Drance, Official Site. https://www.nant-de-drance.ch/

Pan, E., Amadei, B. & Savage, W. 1995: Gravitational and tectonic stresses in anisotropic rock with irregular topography. International Journal of Rock Mechanics and Mining Sciences & Geomechanics Abstracts 32(3):201–214, DOI 10.1016/0148-9062(94)00046-6, URL https://linkinghub.elsevier.com/retrieve/pii/0148906294000466 .

Reiter, K. & Heidbach, O. 2014: 3-D geomechanical–numerical model of the contemporary crustal stress state in the Alberta Basin (Canada). Solid Earth 5, DOI 10.5194/se-5-1123-2014 .

Rocscience 2022: 2D and 3D Geotechnical Software — Rocscience Inc., Official Site. https://www.rocscience.com/ .

Savage, WZ. & Morin, RH. 2002: Topographic stress perturbations in southern Davis Mountains, west Texas 1. Polarity reversal of principal stresses. Journal of Geophysical Research: Solid Earth 107(B12):ETG 5–1–ETG 5–15, DOI https://doi.org/10.1029/2001JB000484 , URL https://agupubs.onlinelibrary.wiley.com/doi/abs/10.1029/2001JB000484 , https://agupubs.onlinelibrary.wiley.com/doi/pdf/10.1029/2001JB000484

Sonney, R. 2007 : Système hydrthoermal de Lavey-les-Bains: évolution des paramètres physiques et chimiques de l'eau thermale avec la production. p 113

swissALTI3D 2022 : Office fédéral de topographie swisstopo. https://www.swisstopo.admin.ch/fr/geodata/height/alti3d.html

Valley, BC. 2007: The relation between natural fracturing and stress heterogeneities in deep-seated crystalline rocks at Soultz-sous-Forêts (France). PhD thesis.

Warpinski, N. & Teufel, L. 1991: In situ stress measurements at Rainier Mesa, Nevada test site — Influence of topography and lithology on the stress state in tuff. International Journal of Rock Mechanics and Mining Sciences Geomechanics Abstracts 28(2):143–161, DOI https://doi.org/10.1016/0148-9062(91)92163-S, URL . https://www.sciencedirect.com/science/article/pii/014890629192163S

Zang, A. & Stephansson, O. 2010: Stress Field of the Earth's Crust. Springer Netherlands, Dordrecht, DOI 10.1007/978-1-4020-8444-7, URL http://link.springer.com/10.1007/978-1-4020-8444-7 .

Zoback, MD. 2007: Reservoir Geomechanics. Cambridge University Press, DOI 10.1017/CBO9780511586477

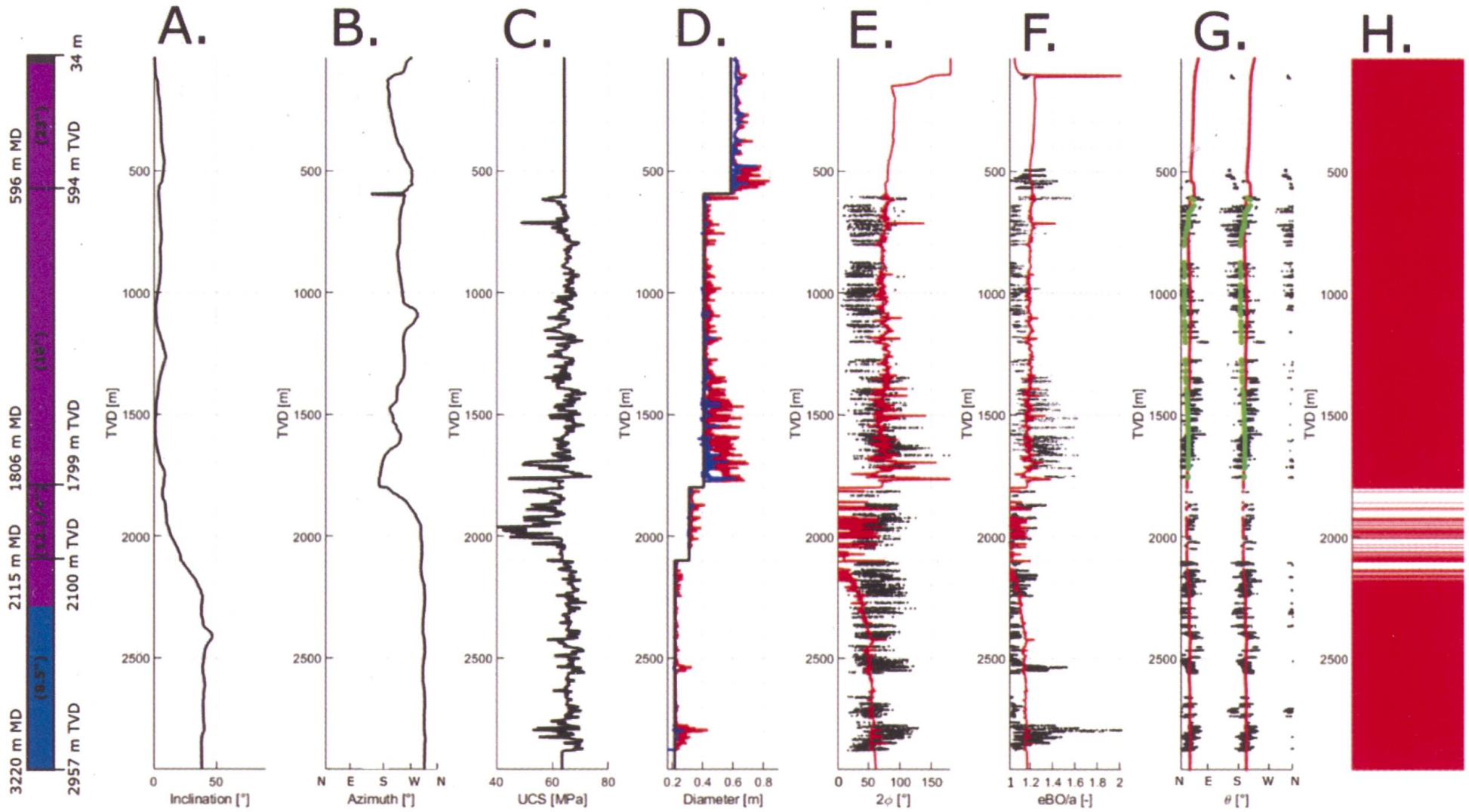

Fig. 6: induced rupture as a result of the stress condition defined by the best-fitted 3D geomechanical numerical model. The simulated rupture (red lines), evaluated in terms of breakouts width 2ϕ normalized breakouts extent *eBO/a* and breakouts azimuth ϑ fits the observed well. A. Borehole deviation; B. Borehole azimuth; C. Uniaxial confined strength [MPa]; D. Well Geometry Instrument overview (the black line represents the BIT size, the red line represents the maximum arm diameter and the blue one the minimum arm diameter); E. Breakouts width 2ϕ (the black dots represent the observed values and the red ones the simulated values from the 3D model best-fitted stress tensor); F. Breakouts normalized extent *eBO/a* (black dots: observed; red dots: simulated); G. Breakouts azimuth ϑ (black dots: observed; red dots: simulated, green dots: average breakouts azimuth observed along the second section (16"); H. Simulated rupture (red intervals).